Canonical Correlation Analysis for Coherent Change Detection in Synthetic Aperture Sonar Imagery

Tesfaye G-Michael* and J. Derek Tucker*
*Naval Surface Warfare Center - Panama City Division
Panama City, Florida 32407-7001
Email: {tesfaye.g-michael, james.d.tucker}@navy.mil

***Abstract*—The application of coherent change detection has enabled the synthetic aperture radar community to identify man-made changes in repeat-pass imagery not detectable in magnitude only images. In a similar manner, CCD may allow synthetic aperture sonar community to identify man-made changes on the seafloor. We propose a coherent change detection scheme using canonical correlation analysis to determine the linear dependence between the canonical coordinates of the input channels, which are represented by baseline and repeat survey pass of the synthetic aperture sonar. We demonstrate the versatility of this method with application to a synthetic aperture sonar imagery data set with identical trajectory and modest scene change.**

***Index Terms*—canonical correlation analysis, coherent change detection, synthetic aperture sonar**

I. Introduction

Battlefield situation awareness is a critical requirement for the success of future combat operations. Sensors provide us with the data of various threat activities in the areas of interest. The all-weather, high-resolution, advanced Synthetic Aperture Sonar (SAS) imagery systems form an ideal sensor that provides two-dimensional sonar images of stationary sea floor targets which would be not only used for detection but also for target classification. Detecting a cue that threat activities have taken place by monitoring the bottom disturbances that are left behind (e.g. sand disturbance during target placement) provides valuable information. Once the changes in the sonar imagery are detected, specific high resolution sensors could be deployed or steered in the surveillance areas for the better imaging of the targets of interest. Also, from the sequence of the detected change features it is even possible to back-track and locate the origin of the targets and their behavior.

Coherent Change Detection (CCD) is the process of detecting changes from pairs of SAS images of approximately the same location observed at two different instances. The problem of CCD and subsequent anomaly feature extraction is complicated due to several factors such as the presence of random speckle pattern in the images, changing environmental conditions, and platform instabilities. These complications make the detection of weak target activities even more difficult. Typically [1], the degree of similarity between two images measured at each pixel locations is the coherence between the complex pixel values in the two images. Higher coherence indicates little change in the scene represented by the pixel and lower coherence indicates change activity in the scene. Such coherence estimation scheme based on the pixel intensity correlation is an ad-hoc procedure where the effectiveness of the change detection is determined by the choice of threshold which can lead to high false alarm rates. Extracting quality, useful and representative change features from CCD imagery that were induced due to human activities is extremely important. However, this problem is complicated due to the factors discussed above. Repetitive activities, like tide and sand ripple changes will create repetitive change activities that are of less significance. High false alarm in change detection due to such repetitive activities is another major problem. Also, the presence of weak threat activities will create small change information and extracting meaningful change information in such situations are very difficult.

Recently, coherent change detection has been employed by Corr in [1] for monitoring the urban area development using synthetic aperture radar (SAR) data where the similarity between two SAR images is calculated based on the coherence function [2] where the change detection involves a decision logic based upon a coherence measurement at a particular position. This procedure is based on the idea that pixel locations corresponding to unchanged activities will have high coherence and change activities are usually perceived with low coherence. Corr also utilized the same CCD method to detect vehicle movements in [3]. The limitations in these systems is that the detection performance is vastly affected by the choice of the threshold. Moreover, detection of different objects would require different levels of threshold setting. In [4], CCD and coherent change feature extraction of two multi-spectral satellite image data was performed using the multivariate alteration detection (MAD) and maximum autocorrelation factor (MAF). The MAD transformations accurately detect coherent patterns of the temporal changes. MAF analysis is a transformation in which the new coordinates maximizes the autocorrelations between the neighboring pixels. The MAF of the MAD are computed to provide a way to retain the spatial context of the neighborhood pixels. It has also been shown that both the MAD and MAD/MAF are superior to the principal component analysis (PCA) transformation of the simple differenced data in capturing the coherent change features. In [5] PCA is employed to detect the temporal

changes between two remote sensing multi-spectral satellite images of a plutonium production facility. The changes in the production facility due to construction activities and other factors are well captured and also shows that the principle coordinates could form a useful feature in representing the coherent change patterns.

One coherent change detection method that has not been explored for SAS imagery is canonical correlation analysis (CCA). This method has shown great promise in underwater target detection classification problems using sonar backscatter [6]–[9]. The canonical coordinate analysis method determines linear dependence [10] or coherence between two data channels. This method not only determines the amount of dependence or independence between two data channels (e.g. two sonar images) but also extracts, via the canonical correlations, a subset of the most coherent features for classification purposes. Canonical coordinate analysis allows us to quantify the changes between the returns from the bottom and when target activities are present and at the same time extract useful features for target classification.

In this paper, a new coherent change detection method for high-resolution synthetic aperture sonar imagery is developed using CCA as a change detection tool and a feature extraction process. In both cases, the canonical correlations are formed between two sonar images from repeat passes over the ocean floor. From these canonical correlations, coherence (or incoherence) can be measured and used to determine what has changed between the two sonar images. The data used in this study was provided by the NSWC PCD in Panama City, FL. The data set consists of high-resolution synthetic aperture sonar images with repeat surveillance passes where target changes introduced.

This paper is organized as follows: Section II reviews the CCA method and its application as a feature extraction tool. Section III develops the method for CCD using CCA. In Section IV, the coherent change detection results of using CCA to detect changes in sonar imagery are presented. Finally, conclusions and observations are made in Section V.

II. Review of Canonical Coordinate Analysis

Canonical correlation analysis was developed by Hotelling as a procedure for assessing the relationship between two sets of variables [11]. As the name implies, CCA quantifies the relationship with correlation coefficients and the term "canonical" relates to the coordinate system in which the correlation is measured. This coordinate system reveals the relationships between the two sets of variables optimally from a correlation point of view. The language and terminology used in this section is taken mostly from [10], [12].

Consider the composite data vector $\mathbf{z}$ consisting of two random vectors $\mathbf{x} \in \mathbb{C}^m$ and $\mathbf{y} \in \mathbb{C}^n$, i.e.

$$\mathbf{z} = \begin{bmatrix} \mathbf{x} \\ \mathbf{y} \end{bmatrix} \in \mathbb{C}^{(m+n)}. \tag{1}$$

For the remainder of the derivations, it is assumed that $m \geq n$, also the notation $(\cdot)^H$ represents the Hermitian operation. Assume that $\mathbf{x}$ and $\mathbf{y}$ have zero means and share the composite covariance matrix

$$\begin{aligned} R_{zz} = E[\mathbf{z}\mathbf{z}^H] &= E\left[\begin{pmatrix} \mathbf{x} \\ \mathbf{y} \end{pmatrix} \begin{pmatrix} \mathbf{x}^H & \mathbf{y}^H \end{pmatrix} \right] \\ &= \begin{bmatrix} R_{xx} & R_{xy} \\ R_{yx} & R_{yy} \end{bmatrix}. \end{aligned} \tag{2}$$

If $\mathbf{x}$ and $\mathbf{y}$ are now replaced by their corresponding whitened vectors, then the composite vector $\boldsymbol{\xi}$ is

$$\boldsymbol{\xi} = \begin{bmatrix} \boldsymbol{\zeta} \\ \boldsymbol{\nu} \end{bmatrix} = \begin{bmatrix} R_{xx}^{-1/2} & \mathbf{0} \\ \mathbf{0} & R_{yy}^{-1/2} \end{bmatrix} \begin{bmatrix} \mathbf{x} \\ \mathbf{y} \end{bmatrix}, \tag{3}$$

where $R_{xx}^{1/2}$ is a square-root of R_{xx} with $R_{xx}^{1/2} R_{xx}^{H/2} = R_{xx}$ and $R_{xx}^{-1/2} R_{xx} R_{xx}^{-H/2} = \mathrm{I}$. The covariance matrix of $\boldsymbol{\xi}$ may be written as

$$\begin{aligned} R_{\xi\xi} = E[\boldsymbol{\xi}\,\boldsymbol{\xi}^H] &= E\left[\begin{pmatrix} \boldsymbol{\zeta} \\ \boldsymbol{\nu} \end{pmatrix} \begin{pmatrix} \boldsymbol{\zeta}^T & \boldsymbol{\nu}^H \end{pmatrix} \right] \\ &= \begin{bmatrix} R_{\zeta\zeta} & R_{\zeta\nu} \\ R_{\nu\zeta} & R_{\nu\nu} \end{bmatrix} \\ &= \begin{bmatrix} \mathrm{I} & \mathrm{C} \\ \mathrm{C}^H & \mathrm{I} \end{bmatrix}, \end{aligned} \tag{4}$$

where

$$\begin{aligned} \mathrm{C} = E[\boldsymbol{\zeta}\boldsymbol{\nu}^T] &= E[(R_{xx}^{-1/2}\mathbf{x})(R_{yy}^{-1/2}\mathbf{y})^H] \\ &= R_{xx}^{-1/2} R_{xy} R_{yy}^{-H/2} \end{aligned} \tag{5}$$

is called the *coherence matrix* of $\mathbf{x}$ and $\mathbf{y}$ [10]. Therefore, the coherence matrix C is the cross-covariance matrix between the whitened versions of $\mathbf{x}$ and $\mathbf{y}$. Correspondingly, the coordinates $\boldsymbol{\zeta}$ and $\boldsymbol{\nu}$ are called the *coherence coordinates*. Now it is possible to determine the singular value decomposition (SVD) of the coherence matrix, namely

$$\begin{aligned} &\mathrm{C} = R_{xx}^{-1/2} R_{xy} R_{yy}^{-H/2} = \mathrm{F}\mathrm{K}\mathrm{G}^H \quad \text{and} \\ &\mathrm{F}^H \mathrm{C}\mathrm{G} = \mathrm{F}^H R_{xx}^{-1/2} R_{xy} R_{yy}^{-T/2} \mathrm{G} = \mathrm{K}, \end{aligned} \tag{6}$$

where $\mathrm{F} \in \mathbb{C}^{m\times m}$ and $\mathrm{G} \in \mathbb{C}^{n\times n}$ are orthogonal matrices [13, Ch. 2.5], i.e.

$$\mathrm{F}^H\mathrm{F} = \mathrm{F}\mathrm{F}^H = \mathrm{I}(m) \quad \text{and} \quad \mathrm{G}^H\mathrm{G} = \mathrm{G}\mathrm{G}^H = \mathrm{I}(n), \tag{7}$$

and

$$\mathrm{K} = \begin{bmatrix} \mathrm{K}(n) \\ \mathbf{0} \end{bmatrix} \in \mathbb{C}^{m\times n} \tag{8}$$

is a diagonal singular value matrix, with $\mathrm{K}(n) = \mathrm{diag}[k_1, k_2, \ldots, k_n]$ and $1 \geq k_1 \geq k_2 \geq \ldots \geq k_n > 0$.

We then use the orthogonal matrices F and G to transform the whitened composite vector $\boldsymbol{\xi}$ into the canonical composite vector $\mathbf{w}$,

$$\begin{aligned} \mathbf{w} &= \begin{bmatrix} \mathbf{u} \\ \mathbf{v} \end{bmatrix} = \begin{bmatrix} \mathrm{F}^H & \mathbf{0} \\ \mathbf{0} & \mathrm{G}^H \end{bmatrix} \begin{bmatrix} \boldsymbol{\zeta} \\ \boldsymbol{\nu} \end{bmatrix} \\ &= \begin{bmatrix} \mathrm{F}^H & \mathbf{0} \\ \mathbf{0} & \mathrm{G}^H \end{bmatrix} \begin{bmatrix} R_{xx}^{-1/2} & \mathbf{0} \\ \mathbf{0} & R_{yy}^{-1/2} \end{bmatrix} \begin{bmatrix} \mathbf{x} \\ \mathbf{y} \end{bmatrix}. \end{aligned} \tag{9}$$

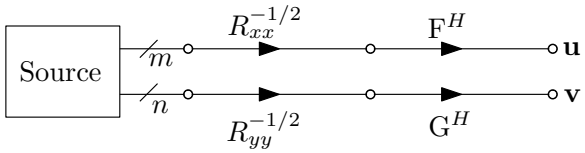

Fig. 1: Transformation from standard coordinates $\mathbf{x}$ and $\mathbf{y}$ to canonical coordinates $\mathbf{u}$ and $\mathbf{v}$.

Then, the covariance matrix for the canonical composite vector $\mathbf{w}$ is obtained as

$$\begin{aligned} R_{ww} &= E[\mathbf{w}\mathbf{w}^H] = E\left[\begin{pmatrix} \mathbf{u} \\ \mathbf{v} \end{pmatrix} \begin{pmatrix} \mathbf{u}^H & \mathbf{v}^H \end{pmatrix} \right] \\ &= \begin{bmatrix} R_{uu} & R_{uv} \\ R_{vu} & R_{vv} \end{bmatrix} = \begin{bmatrix} \mathrm{I} & \mathrm{K} \\ \mathrm{K}^H & \mathrm{I} \end{bmatrix}. \end{aligned} \tag{10}$$

The elements of $\mathbf{u} = [u_i]_{i=1}^m \in \mathbb{C}^m$ are referred to as the *canonical coordinates* of $\mathbf{x}$ and the elements of $\mathbf{v} = [v_i]_{i=1}^n \in \mathbb{C}^n$ are the canonical coordinates of $\mathbf{y}$. The diagonal cross-correlation matrix K,

$$\begin{aligned} K = E[\mathbf{u}\mathbf{v}^H] &= E[(\mathrm{F}^H R_{xx}^{-1/2}\mathbf{x})(\mathrm{G}^H R_{yy}^{-1/2}\mathbf{y})^H] \\ &= \mathrm{F}^H \mathrm{C}\mathrm{G} \end{aligned} \tag{11}$$

is called the *canonical correlation matrix* of *canonical correlations* k_i, with $1 \geq k_1 \geq k_2 \geq \cdots \geq k_n > 0$. Thus, the canonical correlations measure the correlations between pairs of corresponding canonical coordinates. That is, $E[u_i v_j] = k_i \delta_{ij}$; $i \in [1, n]$, $j \in [1, m]$, with δ_{ij} being the Kronecker delta. The canonical correlations k_i are also the singular values of the coherence matrix C. Correspondingly, $\mathrm{K}\mathrm{K}^H$ is the squared canonical correlation matrix of the squared canonical correlations k_i^2. Since F and G are orthogonal matrices, we may write the squared coherence matrix $\mathrm{C}\mathrm{C}^H$ as

$$\begin{aligned} \mathrm{C}\mathrm{C}^H &= R_{xx}^{-1/2} R_{xy} R_{yy}^{-1} R_{yx} R_{xx}^{-H/2} \\ &= \mathrm{F}\mathrm{K}\mathrm{G}^H \mathrm{G}\mathrm{K}^H \mathrm{F}^H = \mathrm{F}\mathrm{K}\mathrm{K}^H \mathrm{F}^H. \end{aligned} \tag{12}$$

This shows that the squared canonical correlations k_i^2 are the eigenvalues of the squared coherence matrix $\mathrm{C}\mathrm{C}^H$, or equivalently, of the matrix $R_{xx}^{-H/2} \mathrm{C}\mathrm{C}^H R_{xx}^{H/2} = R_{xx}^{-1} R_{xy} R_{yy}^{-1} R_{yx}$. It is interesting to note that these eigenvalues are invariant to the choice of a square-root for R_{xx}.

Figure 1 illustrates the transformation from standard coordinates $\mathbf{x}$ and $\mathbf{y}$ to coherence coordinates $\boldsymbol{\zeta}$ and $\boldsymbol{\nu}$ and then to canonical coordinates $\mathbf{u}$ and $\mathbf{v}$. It can be noted that the transformation from standard coordinates $\mathbf{x}$ and $\mathbf{y}$ to canonical coordinates $\mathbf{u}$ and $\mathbf{v}$ can be represented by $\mathbf{u} = \mathrm{W}^H \mathbf{x}$ and $\mathbf{v} = \mathrm{D}^H \mathbf{y}$ where $\mathrm{W}^H = \mathrm{F}^H R_{xx}^{-1/2}$ and $\mathrm{D}^H = \mathrm{G}^H R_{yy}^{-1/2}$. In this case, W and D are known as the canonical mapping matrices.

A. Linear Dependence and Coherence

It can be shown [10] that the linear dependence measure between the two-channels $\mathbf{x}$ and $\mathbf{y}$ is given by

$$L = \det(\mathrm{I} - \mathrm{K}\mathrm{K}^H) = \prod_{i=1}^{n} (1 - k_i^2); \quad 0 \leq L \leq 1, \tag{13}$$

i.e. the linear dependence is represented in terms of the canonical correlations $k_i's$ which measure the dependence between the corresponding canonical coordinates. The measure L takes the value 0 iff there is perfect linear dependence between $\mathbf{x}$ and $\mathbf{y}$; it takes the value 1 iff $\mathbf{x}$ and $\mathbf{y}$ are independent. The i^{th} term of the product on the right hand side of (13), i.e. $(1 - k_i^2)$, measures the linear dependence between the i^{th} canonical coordinate of $\mathbf{x}$ and the i^{th} canonical coordinate of $\mathbf{y}$.

The *coherence* measure between $\mathbf{x}$ and $\mathbf{y}$ is given by

$$\begin{aligned} H = 1 - L &= 1 - \det(\mathrm{I} - \mathrm{K}\mathrm{K}^H) \\ &= 1 - \prod_{i=1}^{n} (1 - k_i^2); \quad 0 \leq H \leq 1. \end{aligned} \tag{14}$$

The channels $\mathbf{x}$ and $\mathbf{y}$ are perfectly coherent iff $H = 1$; and non-coherent iff $H = 0$.

III. Coherent Change Detection using CCA

In this section, we discuss how CCA may be used to capture the change information for coherent change detection. In order to capture the change information for CCD we need to capture the divergence between the two data channels $\mathbf{x}$ or $\mathbf{y}$, i.e. our two SAS images. It can be noted that the subdominant canonical coordinates are the ones that maximize the divergence (or coherent change) between the two channels, under the constraint of maximizing the rate at which the divergence is captured. In other words, the subdominant canonical coordinates of the two channels captures most of the coherent change features between them with a minimum dimensional feature set. For a better understanding on this property of the canonical coordinates, consider the following detection problem. The detection problem is to decide between the two hypothesis $H_0 : \mathbf{x} = \mathbf{s}$ (i.e. image with no change) and the alternative $H_1 : \mathbf{y} = \mathbf{s} + \mathbf{n}$ (i.e. image with change), such that $R_{yy} = R_{xx} + R_{nn}$, where R_{nn} is the covariance matrix of the additive noise (i.e. the change information). In [12], the Neyman-Pearson detector for testing H_0 and H_1 was written as,

$$l(\mathbf{v}) = \mathbf{v}^H ([\mathrm{I} - \mathrm{K}^2]^{-1} - \mathrm{I})\mathbf{v} \tag{15}$$

where $l(\mathbf{v})$ is the log likelihood test that minimizes the risk involved in deciding between H_0 and H_1. The J-divergence, which is a measure of detectability, between H_1 and H_0 is [12],

$$\begin{aligned} J &= E_{H_1} l(\mathbf{v}) - E_{H_0} l(\mathbf{v}) \\ &= tr([\mathrm{I} - \mathrm{K}^2]^{-1} - \mathrm{I} - \mathrm{K}^2) \\ &= \sum_{i=1}^{N} \frac{k_i^4}{1 - k_i^2}. \end{aligned} \tag{16}$$

The function $\frac{k_i^4}{1-k_i^2}$ is non-increasing in the interval (0, 1]. *Consequently the rank-r detector that maximizes the divergence is the detector that uses the subdominant coordinates corresponding to the subdominant canonical correlations* k_i. The divergence between the two hypothesis (or the SAS

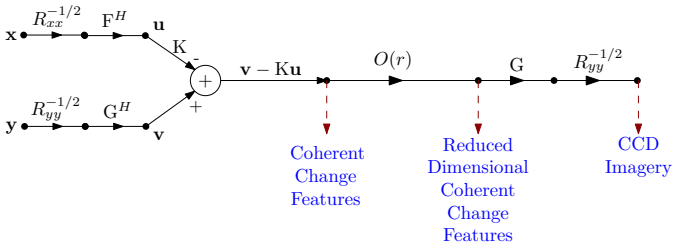

Fig. 2: Coherent change feature extraction and CCD image generation using canonical correlation analysis.

images) considering the r subdominant canonical correlations is,

$$J_r = \sum_{i=r}^{N} \frac{k_i^4}{1-k_i^2}. \tag{17}$$

The coherent change features representing the coherent change information between canonical coordinates $\mathbf{v}$ and $\mathbf{u}$ is $\mathbf{v} - \mathrm{K}\mathbf{u}$ (see Figure 2). We have seen that the subdominant canonical coordinates capture the coherent change information, under the constraint of maximum rate. Thus, retaining the last few components of the difference vector $\mathbf{v}-\mathrm{K}\mathbf{u}$, is enough to capture almost all the change features. This operation can be mathematically expressed as, $O(r)(\mathbf{v} - \mathrm{K}\mathbf{u})$, where $O(r)$ is a $m \times m$ diagonal matrix with diagonal 0 at the first $m-r$ location and 1 at the last r locations. Thus, it can be seen that the coherent change features are extracted without the need to perform an external feature selection. Moreover, one is able to extract the CCD imagery, if required. The CCD image block can be constructed from the coherent change features using the simple linear transformation,

$$\mathbf{e} = R_{yy}^{1/2}\mathrm{G}O(r)(\mathbf{v} - \mathrm{K}\mathbf{u}) \tag{18}$$

In our application to SAS imagery only the last few canonical coordinate pairs and their corresponding canonical correlations make a significant contribution to the coherent change information between the two channels. The conventional canonical coordinate decomposition reviewed in this section requires computation of the square-root inverses of the covariance matrices R_{xx} and R_{yy} followed by the SVD of the coherence matrix C. Moreover, the conventional method does not allow for extraction of a subset of canonical coordinates and correlations. These deficiencies make the conventional method inefficient for decomposition of large dimensional channels in real time applications. In [14], a new algorithm using the *alternating power method* was developed, together with a deflation process, that allows for time- and order-recursive extraction of the canonical coordinates and correlations one-by-one. This iterative algorithm can be used to provide real-time implementation of the canonical coordinate decomposition.

IV. Results

A. Data Description and Pre-Processing

In this section, the CCA method described in Section III is applied to a data set that contains high frequency high resolution synthetic aperture sonar images with multiple passes over the same region with targets inserted between the passes. More information on high-resolution synthetic aperture sonars can be found in [15], [16]. The raw sonar data is first preprocessed by applying a grazing angle compensation (GAC) [17]. Grazing angle compensation is a aperture invariant imaging technique that uses estimates of bottom grazing angles to correctly project temporally sampled data onto a seafloor grid. This is done to adjust for changes in grazing angle between repeat passes of the sonar. The sonar images in this data set are complex and are generated at the output of a k-space or wavenumber beamformer [18], [19, Ch. 6.2], which computes the 2-D Fourier transform of the raw or range-compressed sonar data in the delay-time/aperture domain. This converts the data into the spatial frequency/wavenumber (ω, k)-domain where it is multiplied by the power spectrum of the transmitted wavefront. A change of variables is done by Stolt interpolation [20]. This change of variables maps the frequency/wavenumber (ω, k)-domain into the wavenumber domain (k_x, k_y). The inverse 2-D Fourier transform is then taken of the mapped data to form the complex image. For more information on the k-space/wavenumber beamformer the reader is referred to [19, Ch. 6].

Next, the first SAS image is partitioned into blocks of size $m \times m$ to form the realization of the random process that represents the $\mathbf{x}$-channel, these blocks are reshaped into column vectors and inserted into a sample data matrix. This process is also repeated for the second pass SAS image to form realizations of the $\mathbf{y}$-channel. Using the sample data matrices the canonical coordinates and correlations are then extracted from the two channels. Using the canonical coordinates and correlations the coherent change information between th two images is formed via $\mathbf{v} - \mathrm{K}\mathbf{u}$ (see Figure 2). Moreover, the extracted canonical correlations can be used as a feature vector in a subsequent classification step to classify the changes. This feature vector represents statistical information about the change between the two images.

B. Coherent Change Detection Performance

This section presents the different results obtained with applying CCA for CCD described in the previous sections. First, results obtained using the grazing angle compensation will be shown in Figure 3, and then those produced without GAC will be presented in Figure 4. We will also study the particular differences between the different algorithms and the influence of corresponding parameters for these techniques. Figure 3a presents the first pass over the target field with the sonar traveling at a altitude of 5 meters and Figure 3b presents the second pass over the target field with the sonar traveling at an altitude of 4.8 meters and a baseline of 0.2 meters. The difference between the two passes is that a cylinder shaped target was inserted into the target field at a range of 800 pixels in Figure 3b.

To apply CCA, the two SAS images in Figure 3a and 3b are partitioned in into non-overlapping blocks of size 5 x 5. Thus, the length of the input data vector is 25 and the 25 x 1 vectors

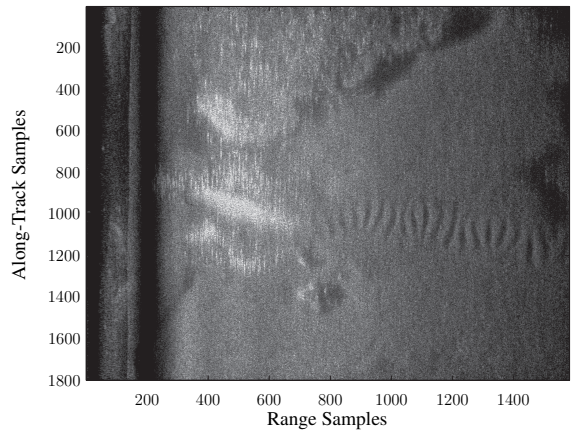

(a) First Pass SAS Image

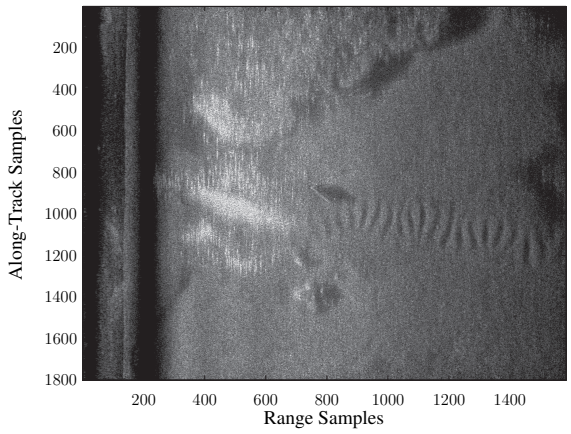

(b) Repeat Pass SAS Image with an Object

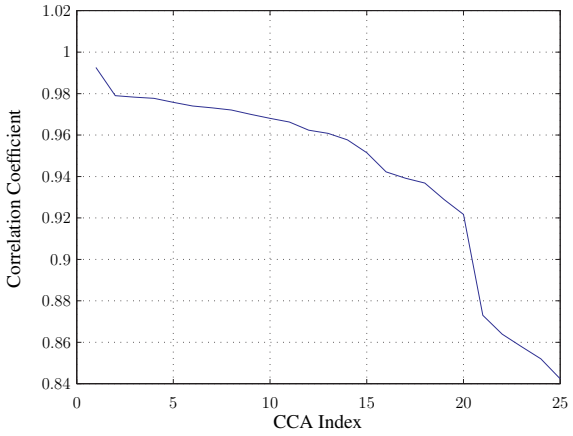

(c) Canonical Correlations

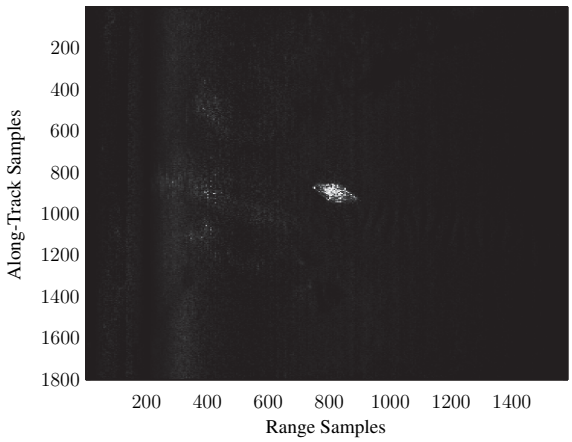

(d) Difference Image

Fig. 3: Coherent change detection using CCA with GAC.

to the two images become realization of the random process $\mathbf{x}$ and $\mathbf{y}$. Canonical coordinate analysis is performed on this two-channel data and the coherent change vectors $O(r)(\mathbf{v} - \mathrm{K}\mathbf{u})$ are obtained. First, we applied the method to the grazing angle compensated data with the canonical correlations ($\mathbf{k}$) presented in Figure 3c. It can be noted that the first 20 canonical correlations are sufficiently close to one representing the coherent information between $\mathbf{x}$ and $\mathbf{y}$ and they begin to drop off in value for the 21^{st} and larger correlation. From this we chose only to retain the last 5 correlations in forming our difference image as the pertain to the incoherence between $\mathbf{x}$ and $\mathbf{y}$. The difference image that are formed using equation (18) with the last 5 canonical correlations is presented in Figure 3d. With only just 5 correlations we are able to accurately capture the target which was placed in-between passes with no false alarm from the ocean change.

We conducted a second test to see how our algorithm would perform without applying the GAC technique. Moreover, this would test our algorithms robustness to changes in the platform instability. The canonical correlations for the data without GAC is presented in Figure 4a. It is interesting to note here that we have a more rapid fall off the correlations than in Figure 3c due the removal of GAC. However, still have a dramatic change between the last 9 and correlations the first 16. Therefore, we chose to retain the last 9 correlations to form the difference image using equation (18) and the difference image is presented in Figure 4b. Again we pickup the target which is the dominant feature in the difference image, but we pick up a few false alarm changes near the vehicle which are due to the change in pixel intensity and phase for the lowering of the sonar platform. However, the magnitudes of those changes are still less than target and could be suppressed by thresholding the image.

It is clear that with GAC the images exhibit a good correlation though at the cost of a more complex image formation procedure. Indeed, when using GAC, projecting the slant range onto the ground range, it has a strong impact on the amplitude and phase of the SAS image. The grazing angle compensated

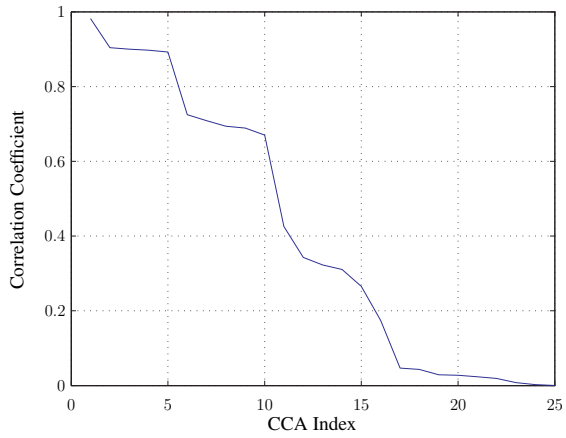

(a) Canonical Correlations

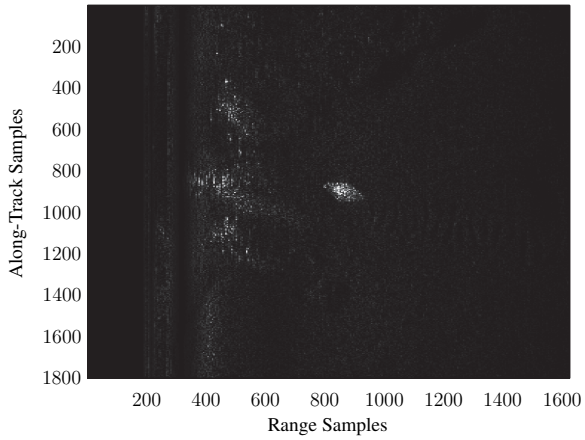

(b) Difference image

Fig. 4: Coherent change detection using CCA without GAC.

areas are brighter on the image because the resolution cells are larger, hence more power is backscattered toward the SAS causing the incident angle to be steeper. The area imaged in each SAS resolution cell depends on the sea floor topography and the sea floor terrain slope in the plane perpendicular to the range direction, and on the terrain slope in the along-track (azimuth) direction. With either type of image formation we were able to capture the difference in the images with high fidelity while also extracting via the canonical correlations a feature vector of the coherent change information.

V. Conclusion

In this paper, CCA was used as a coherent change detection tool to detect changes in repeat pass synthetic aperture sonar imagery. The basic idea is that when an object (target) is present in a repeat pass sonar image there will be a change in the coherence level compared to the case when there is no object. Further it has been shown that using the subdominant canonical correlations a difference image can be performed and features can be extracted for the coherent change. Our experiments on the data set provided by the NSWC PCD demonstrated that CCD using CCA method provided good change detection results while keeping the false alarm low. Thus, CCA shows great promise as a coherent change detection tool in SAS imagery.

Acknowledgment

This work was supported by the NSWC PCD In-house Laboratory Independent Research program funded by the Office of Naval Research[1].

References

[1] D. G. Corr, "Coherent change detection for urban development monitoring," *IEE Colloquium on Radar Interferometry*, vol. 11, pp. 6/1 – 6/6, April 1997.

[2] ——, "Automatic change detection in spaceborne SAR imagery," *AGARD Conference Proceedings*, pp. 39–1 to 39–7, Oct 1999.

[3] D. G. Corr and A. Rodrigues, "Coherent change detection of vehicle movements," *IEEE Intl. Proc. on Geoscience and Remote Sensing*, vol. 5, pp. 2451 – 2453, July 1998.

[4] A. A. Nielsen, K. Conradsen, and J. J. Simpson, "Multivariate alteration detection (MAD) and MAF post-processing in multispectral, bi-temporal image data: new approaches to change detection studies," *Remote Sensing of Environment*, pp. 1–19, 1998.

[5] I. Niemeyer, M. Canty, and D. Klaus, "Unsupervised change detection techniques using multispectral satellite images," *IEEE Intl. Symposium on Geoscience and Remote Sensing*, vol. 1, pp. 327 – 329, July 1999.

[6] J. D. Tucker, M. R. Azimi-Sadjadi, and G. J. Dobeck, "Coherent-based method for detection of underwater objects from sonar imagery," *Proc. SPIE*, vol. 6553, pp. U1–U8, April 2007.

[7] ——, "Canonical coordinates for detection and classification of underwater objects from sonar imagery," *Proc. of IEEE OCEANS 2007 Conference Europe*, pp. 1–6, June 2007.

[8] M. R. Azimi-Sadjadi and J. D. Tucker, "Target detection from dual disparate sonar platforms using canonical correlations," *Proc. SPIE*, vol. 6953, pp. J1 – J10, March 2008.

[9] N. Wachowski and M. R. Azimi-Sadjadi, "Buried underwater target classification using frequency subband coherence analysis," *Proc. of MTS/IEEE Oceans 2008 Conference*, pp. 1–8, Sep 2008.

[10] L. Scharf and C. Mullis, "Canonical coordinates and the geometry of inference, rate, and capacity," *IEEE Transactions on Signal Processing*, vol. 48, no. 3, pp. 824–891, March 2000.

[11] H. Hotelling, "Relations between two sets of variates," *Biometrika*, vol. 28, pp. 321–377, 1936.

[12] A. Pezeshki, L. L. Scharf, J. K. Thomas, and B. D. Van Veen, "Canonical coordinates are the right coordinates for low-rank Gauss-Gauss detection and estimation," *IEEE Trans. Signal Process.*, vol. 54, no. 12, pp. 4817–4820, Dec 2006.

[13] G. H. Golub and C. F. Van Loan, *Matrix Computations*, Third ed. Johns Hopkins University Press, 1996.

[14] A. Pezeshki, L. L. Scharf, M. R. Azimi-Sadjadi, and Y. Hua, "Two-channel constrained least squares problems: Solutions using power methods and connections with canonical coordiates," *IEEE Trans. Signal Process.*, vol. 53, no. 1, pp. 121–135, Jan 2005.

[15] N. A. Rimski-Korsakov, Y. S. Russak, and R. B. Pavlov, "Simple digital system for side-scan sonar data imaging," *Proc. of MTS/IEEE Oceans 1994 Conference*, vol. 1, pp. 643–645, Sept 1994.

[16] W. H. Key, "Side scan sonar technology," *Proc. of MTS/IEEE Oceans 2000 Conference*, vol. 2, pp. 1029–1033, Sept 2000.

[17] R. Rikoski and D. Brown, "Holographic Navigation," *IEEE Inter. Conference on Robotics and Automation*, pp. 73–80, May 2008.

[18] R. Bamler, "A comparison of range-Doppler and wavenumber domain SAR focusing algorithms," *IEEE Trans. on Geoscience and Remote Sensing*, vol. 30, no. 4, pp. 706–713, 1992.

[19] M. Soumekh, *Synthetic Aperture Radar Signal Processing*. Wiley, 1999.

[20] R. H. Stolt, "Migration by Fourier transform," *Geophysics*, vol. 43, no. 1, pp. 23–48, 1978.

[1] Approved for public release; distribution unlimited.